higher in the media collected from NP cells cocultured, allowing cell-to-cell contact. Compared with the conventional NP cell-activation method, the coculture system allowing intercellular adhesion with MSCs led to a marked increase in NP cell proliferation, DNA synthesis, and proteoglycan synthesis. A possible explanation is the increased secretion of various cytokines into the culture medium because of the direct contact with MSCs, which act as feeder cells.

In a preliminary study at the author's laboratory, NP cells activated by coculture that allows intercellular contact (Fig. 1) were implanted in an in vivo rabbit model of IVD degeneration.[18] The severity of degeneration was determined over time according to Nishimura's histologic classification. The severity of degeneration was compared between cells treated with the new and conventional methods of activation. The Nishimura grade 24 weeks after transplant was 0 in the normal control group without degeneration induction, 2.8 (the most severe degeneration) in the control group with no treatment, 2.2 in the group receiving NP cells activated by conventional coculture with AF cells, 1.8 in the group receiving NP cells activated by conventional coculture with MSCs, and 1.2 in the group receiving NP cells activated by coculture involving contact with MSCs, the smaller value reflected a significantly less degree of degeneration.

The positive results of this coculture system have been extended to preclinical studies using human cells. Watanabe and colleagues[19] showed that human NP cells obtained from surgery and cocultured with MSCs of the same patient demonstrate up-regulated cellular proliferation and matrix synthesis, as described in animal models.

Strassburg and colleagues[20] demonstrated in the same coculture system using degenerate and nondegenerate NP cells that cellular interactions between MSCs and degenerate NP cells may stimulate both MSC differentiation to an NP-like phenotype and the endogenous NP cell population to regain a nondegenerate phenotype, which consequently increases matrix synthesis for self-repair.

INDUCING STEM CELLS TOWARD THE INTERVERTEBRAL DISK CELL PHENOTYPE

Using the multipotent differentiation capacity of stem cells, the author attempted to induce MSC differentiation in a mixed coculture system with NP or AF cells in alginate beads (Fig. 2). IVD tissue was retrieved during surgery for a burst fracture in a 19-year-old man. Under a microscope, the tissue was separated approximately into the NP and inner and outer AF. The separated tissue was digested with 0.02% pronase (Sigma) and 0.0125% collagenase P (Roche) for 8 hours to obtain cells for primary culture. The NP, inner AF, and outer AF cells were cultured and passaged twice and labeled with PKH26 red fluorescent dye (Sigma). Human MSCs were obtained commercially (Cambrex) and genetically labeled with green fluorescent protein (GFP) by infection with a retrovirus vector. The NP, inner AF, or outer AF cells were cocultured with MSCs in alginate beads in a 50:50 ratio at a density of 30,000 cells/bead. The cells were cocultured for 3 weeks in DMEM + 10% fetal bovine serum, and the cells were recovered. The recovered cells were analyzed, and GFP-positive MSCs were separated by flow cytometry (BD FACSVantage). Characterization of the recovered MSCs by flow cytometry showed that, in forward scatter analysis, the size of MSCs changed markedly after the coculture. MSCs cocultured with NP cells showed significantly greater average cell size, whereas cells cocultured with inner or outer AF cells had a smaller average cell size. The internal complexity analyzed by side scatter showed that MSCs cocultured with NP cells became more complex and that MSCs cocultured with inner or

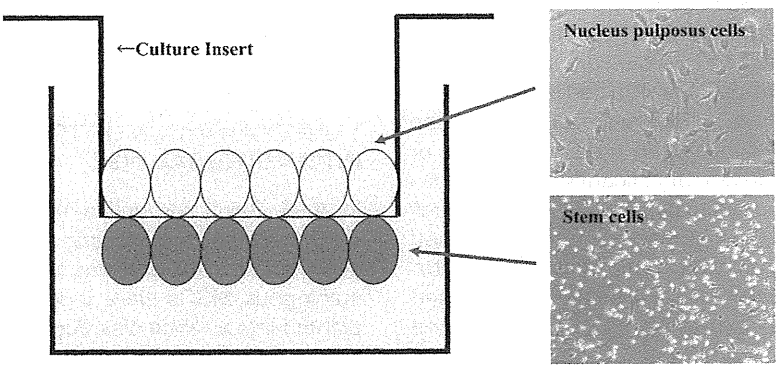

Fig. 1. Use of stem cells as feeder cells for up-regulation of NP cell metabolism. Coculture system allowing cell-to-cell contact.

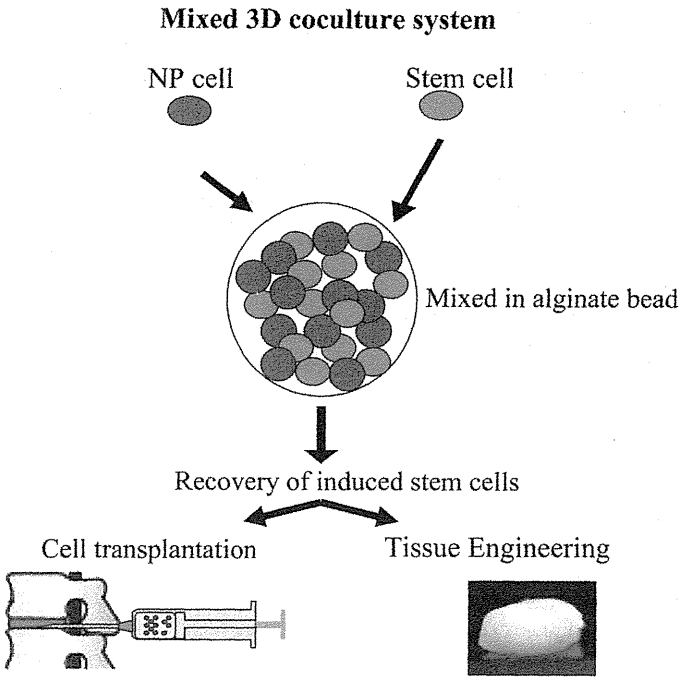

Fig. 2. Use of stem cells for direct induction toward NP phenotype.

outer AF cells became less complex. These characteristics reflected the NP or inner or outer AF cell phenotype of the cocultured opponent. MSCs cocultured with NP cells expressed type II collagen and keratin sulfate, whereas the expression of type I collagen was more intense in cells cocultured with outer AF cells compared with the MSCs before coculture. Gene expression analysis by reverse transcription–polymerase chain reaction (RT-PCR) also confirmed that coculture with different IVD cells in the same 3-D environment led to differentiation of MSCs toward the direction of the cocultured opponent. These experiments showed that the mixed coculture system in alginate is an effective tool for inducing differentiation to MSCs.

Korecki and colleagues[21] hypothesized that MSCs can be differentiated toward the NP cell phenotype if cultured with notochordal cell-conditioned medium. This medium was prepared from notochordal cells maintained in serum-free medium for 4 days. MSCs were cultured in the notochordal cell-conditioned medium, control, or chondrogenic medium. Significantly greater glycosaminoglycan accumulation was found in cell pellets treated with notochordal cell-conditioned medium compared with other media. The notochordal-conditioned medium treatment increased collagen III gene expression. There was a trend for increased expression of laminin-β1 and decreased expression of Sox9 and collagen II relative to the TGF-β group.

Chen and colleagues[22] cocultured synovium-derived stem cells and NP cells in a serum-free pellet system treated with varying doses of TGF-β. The coculture of synovium-derived stem cells and NP cells in a pellet system displayed similar differentiation properties to those of NP cells alone (high levels of collagen II, aggrecan, and Sox9; low level of collagen I; and no collagen X) when treated with high doses of TGF-β1. The coculture and NP cells alone shared a similar higher ratio of aggrecan to collagen II. Hypoxia-inducible factor 1α (HIF-1α) was also up-regulated in the cocultured pellets at day 7 and decreased by day 14 with the time of pellet tissue maturation. The rationale for these in vitro induction methods aims at providing the opportunity to study the cell differentiation pathways of IVD and stem cells and conditioning stem cells before transplantation into the degenerated disk.

TRANSPLANTATION OF STEM CELLS INTO THE INTERVERTEBRAL DISK

In 2003, Sakai and colleagues[23] first reported on transplantation of MSCs into a rabbit disk degeneration model. In the following study, the transplanted autologous MSCs were tagged with GFP, transplanted into a rabbit disk degeneration model, and followed for 48 weeks MRI and radiography.[24,25] Immunohistochemistry was performed to assess the expression of chondroitin sulfate; keratin

sulfate; types I, II, and IV collagen; HIF-1α and HIF-1β and HIF-2α and HIF-2β; glucose transporter (GLUT)-1 and GLUT-3; and matrix metalloproteinase (MMP)-2. They also applied RT-PCR to quantify the expression levels of the genes for aggrecan, versican, types I and II collagen, interleukin (IL)-1β, IL-6, tumor necrosis factor (TNF)-α, MMP-9, and MMP-13. MRI and radiographic results confirmed the regenerative effects of the procedure. GFP-positive cells were detected in the nucleus throughout the study. The percentage of positive cells increased from 21% ± 6% at 2 weeks to 55% ± 8% at 48 weeks; this increase proved that the MSCs survived and proliferated. Immunohistochemistry showed positive staining of all proteoglycan epitopes and type II collagen in some of the GFP-positive cells. MSCs expressed HIF-1α, MMP-2, and GLUT-3, and this phenotypic activity was compatible with that of NP cells. RT-PCR showed significant restoration of aggrecan, versican, and type II collagen gene expression, and significant suppression of TNF-α and IL-1β genes in the transplantation group. These results show that MSCs transplanted into degenerating disks in vivo can survive, proliferate, and differentiate into cells that express the phenotype of NP cells but suppressed inflammatory genes.

Since the first report using the rabbit model in 2003, various animal studies have demonstrated the feasibility of transplantation of MSCs into the IVD and regenerative effects. Crevensten and colleagues[26] used a 15% hyaluronan gel as a carrier and injected fluorescently labeled MSCs into rat coccygeal disks. Although the number of retained MSCs decreased significantly during the first 2 weeks after injection, the initial cell number was restored after 4 weeks and cell viability and disk height were maintained. These results indicate that the injected cells started to proliferate within the rat disk. Zhang and colleagues[27] implanted allogeneic MSCs containing the marker gene LacZ from young rabbits into rabbit IVDs to determine the potential of this cell-based approach. The transplanted allogeneic MSCs survived and increased the proteoglycan content within the disk, an observation that supports the use of these cells as a potential treatment for IVD degeneration. Hiyama and colleagues[28] confirmed the effectiveness of transplantation of MSCs in large animal models, such as chondrodystrophoid breed canines given a nucleotomy, which have closer morphological features of the human IVD compared to other animals to humans. They also showed that transplanted MSCs expressed FasL after transplantation into the NP region, suggesting the preservation of immune privilege in the transplanted MSCs. These findings are to some extent similar to the results of rabbit studies that used primarily notochordal NP cells.

Leung and colleagues[29] investigated allogeneic transplantation of MSCs and reported multiple advantages of such transplantation for treating disk disease. They reasoned that if the NP is an immune-privileged environment, then by presenting less antigen, MSCs should be able to escape alloantigen recognition. Moreover, xenogeneic transplantation of bone marrow MSCs has also been investigated in rats and porcine models and was proved effective.[30,31]

MSCs from other sources have also been studied. MSCs from adipose tissue have been reported as another potential cell source. Adipose tissue is considered an abundant, expendable, and easily accessible source of MSCs. The use of these cells may eliminate the need for in vitro expansion, which raises the possibility of a 1-step regenerative treatment method. Hoogendoorn and colleagues[32] reported that adipose-derived MSCs may be beneficial for cell therapy for IVD disease because they are isolated more easily than are bone marrow MSCs. Ganey and colleagues[33] studied the efficacy of autologous adipose tissue–derived stem cells in promoting disk regeneration in a canine disk injury model and found improved disk matrix production and overall disk morphology. Partial nucleotomy was performed at 3 lumbar levels, and the animals were allowed to recover for 6 weeks before receiving either adipose-derived stem cells in hyaluronic acid carrier, hyaluronic acid alone, or no treatment. The 3 experimental disks plus the 2 adjacent control disks were assessed for up to 12 months. The disks that received the adipose-derived cells more closely resembled the healthy controls, as evidenced by the matrix translucency, compartmentalization of the AF, and cell density within the NP. Matrix analysis of type II collagen and aggrecan demonstrated superior regenerative stimulation in the disks treated with adipose stem cells compared with the carrier-only group or no treatment group.

MSCs were recently transplanted into the human IVD to test their potential to regenerate the degenerated disk. Yoshikawa and colleagues[34] transplanted autologous bone marrow MSCs into IVDs showing vacuum phenomenon and instability in two patients going under decompression surgery for spinal stenosis. The MSCs were cultured in medium containing autogenous serum. During surgery, fenestration was performed on the stenosed spinal canal, and pieces of collagen sponge containing autologous MSCs were then grafted percutaneously to the degenerated IVD. Two years after surgery, radiography and CT showed

improvements in the vacuum phenomenon in both patients. T2-weighted MRI showed high signal intensity in the IVDs with cell grafts, indicating high moisture content. Roentgenkymography showed less lumbar disk instability.

LIMITATIONS AND TASKS FOR THE FUTURE

It is no question that biologic therapies will take over many of the current therapeutics in the field of orthopaedic surgery. The forerunners are the growth factors and application of bone morphogenetic proteins (BMPs), and in clinical trials, have demonstrated excellent advantage in achieving bony fusion with spinal fusion surgeries compared to autologous bone graft. Recently, however, there have been many reports on serious side effects caused by the use of BMPs with spine surgery.[35] These include inflammatory reactions, adverse back and leg pain events, radiculitis, retrograde ejaculation, urinary retention, bone resorption, and implant displacement. This fact warns all health care providers the pitfall of uncontrolled and underestimated use of biologics.

Feasibility in clinical use of stem cells has historically investigated in hematology/oncology field and has spread to different organs and thus, may lead us to be optimistic of potential side effects, however, cautions need to be seriously warranted. Although many animal studies and recent clinical trials have used stem cells in the treatment of IVD degeneration (Fig. 3), careful attention is needed in its application. An experimental study by Vadala et al. has warned using the rabbit model that cell leakage after MSC injection to the IVD may cause osteophyte formation.[36] As they suggest, considerations on cell carriers or annulus-sealing techniques may need to be assessed or perhaps, post-surgical rehabilitation protocols shall be investigated to minimize the leakage. Unintended differentiation and tumorigenesis is another potential risk that stem cell therapy usually faces. More precise definition of IVD cells and their characteristics are needed to understand better how to control the induction pathways. The criteria for successful application need careful investigation in the context of stem cell transplantation into humans.

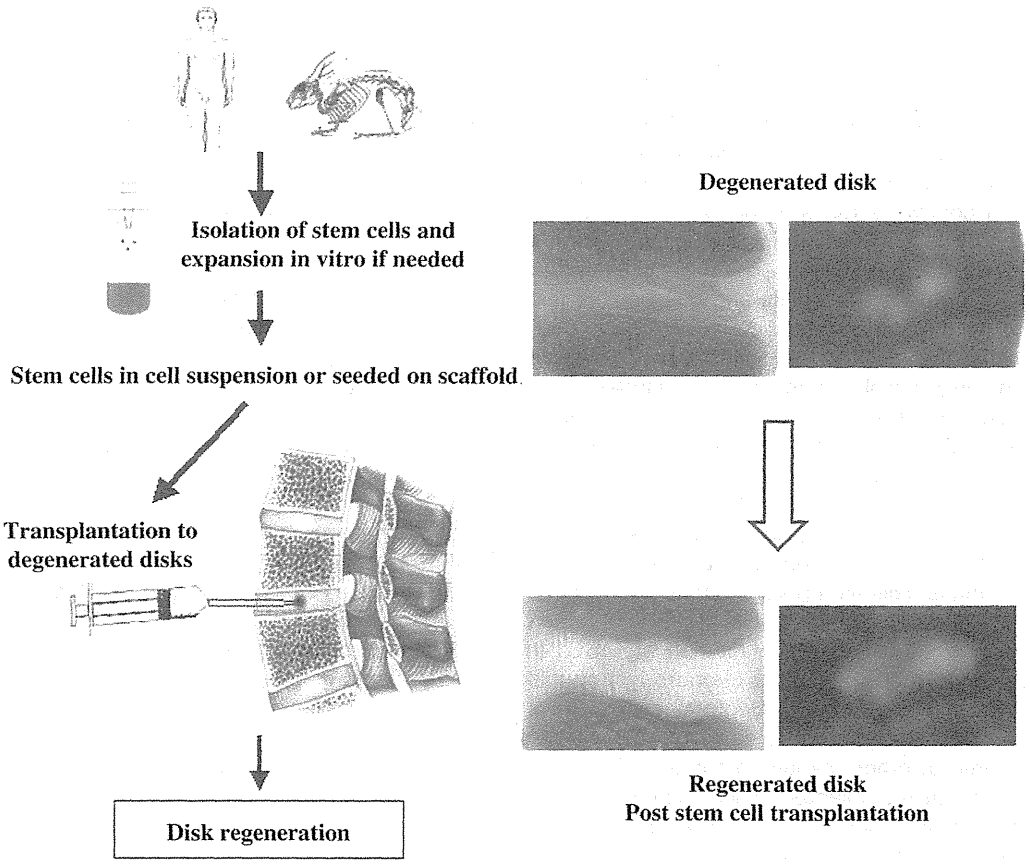

Fig. 3. Use of stem cells in a direct transplantation to degenerated IVD.

Much of the research on stem cell transplantation into the IVD focuses on regeneration of the NP rather than the AF or the vertebral end plate, probably because the NP is a cavity, which eases the application of stem cells. However, further understanding of methods to regenerate the AF and end plate is needed because end plate regeneration is important for securing the nutrition of the IVD microenvironment.

Despite all the limitations and risks, carefully designed clinical trials with appropriate informed consent are the only solution to find the answer and to define whether stem cell therapy will benefit patients with intervetrbral disk degeneration.

REFERENCES

1. Frymoyer JW, Cats-Baril WL. An overview of the incidence and costs of low back pain. Orthop Clin North Am 1991;22:263–71.
2. Deyo RA, Weinstein JN. Low back pain. N Engl J Med 2001;344:363–70.
3. Maniadakis N, Gray A. The economic burden of back pain in the UK. Pain 2000;84:95–103.
4. Buckwalter JA. Aging and degeneration of the human intervertebral disc. Spine 1995;20(11): 1307–14.
5. Taylor JR, Twomey LT. The development of the human intervertebral disc. In: Ghosh P, editor. The biology of the intervertebral disc. Boca Raton (FL): CRC Press Inc.; 1988. p. 39–82.
6. Hunter CJ, Matyas JR, Duncan NA. Cytomorphology of notochordal and chondrocytic cells from the nucleus pulposus: a species comparison. J Anat 2004;205(5):357–62.
7. Maroudas A, Stockwell RA, Nachemson, et al. Factors involved in the nutrition of the human lumbar intervertebral disc: cellularity and diffusion of glucose in vitro. J Anat 1975;120(Pt 1):113–30.
8. Marchand F, Ahmed AM. Investigation of the laminate structure of lumbar disc anulus fibrosus. Spine 1990;15(5):402–10.
9. Yu J. Elastic tissues of the intervertebral disc. Biochem Soc Trans 2002;30(Pt 6):848–52.
10. Wuertz K, Godburn K, Neidlinger-Wilke, et al. Behavior of mesenchymal stem cells in the chemical microenvironment of the intervertebral disc. Spine 2008;33(17): 1843–9.
11. Heathfield SK, Le Maitre CL, Hoyland JA. Caveolin-1 expression and stress-induced premature senescence in human intervertebral disc degeneration. Arthritis Res Ther 2008;10(4):R87.
12. Risbud MV, Guttapalli A, Tsai TT, et al. Evidence for skeletal progenitor cells in the degenerate human intervertebral disc. Spine 2007;32(23): 2537–44.
13. Blanco JF, Graciani IF, Sanchez-Guijo FM, et al. Isolation and characterization of mesenchymal stromal cells from human degenerated nucleus pulposus: comparison with bone marrow mesenchymal stromal cells from the same subjects. Spine (Phila Pa 1976) 2010;35(26):2259–65.
14. Feng G, Yang X, Shang H, et al. Multipotential differentiation of human anulus fibrosus cells: an in vitro study. J Bone Joint Surg Am 2010;92(3):675–85.
15. Fujita J, Mori M, Kawada H, et al. Administration of granulocyte colony-stimulating factor after myocardial infarction enhances the recruitment of hematopoietic stem cell-derived myofibroblasts and contributes to cardiac repair. Stem Cells 2007; 25(11):2750–9.
16. Kawada H, Takizawa S, Takanashi T, et al. Administration of hematopoietic cytokines in the subacute phase after cerebral infarction is effective for functional recovery facilitating proliferation of intrinsic neural stem/progenitor cells and transition of bone marrow-derived neuronal cells. Circulation 2006; 113(5):701–10.
17. Yamamoto Y, Mochida J, Sakai D, et al. Upregulation of the viability of nucleus pulposus cells by bone-marrow-derived stromal cells: significance of direct cell-to-cell contact in co-culture system. Spine 2004;29:1508–14.
18. Nishimura K, Mochida J. Percutaneous reinsertion of the nucleus pulposus. An experimental study. Spine 1996;21:1556–63.
19. Watanabe T, Sakai D, Yamamoto Y, et al. Human nucleus pulposus cells significantly enhanced biological properties in a coculture system with direct cell-to-cell contact with autologous mesenchymal stem cells. J Orthop Res 2010;28(5):623–30.
20. Strassburg S, Richardson SM, Freemont AJ, et al. Co-culture induces mesenchymal stem cell differentiation and modulation of the degenerate human nucleus pulposus cell phenotype. Regen Med 2010;5(5):701–11.
21. Korecki CL, Taboas JM, Tuan RS, et al. Notochordal cell conditioned medium stimulates mesenchymal stem cell differentiation toward a young nucleus pulposus phenotype. Stem Cell Res Ther 2010;1(2):18.
22. Chen S, Emery SE, Pei M. Coculture of synovium-derived stem cells and nucleus pulposus cells in serum-free defined medium with supplementation of transforming growth factor-beta1: a potential application of tissue-specific stem cells in disc regeneration. Spine (Phila Pa 1976) 2009;34(12):1272–80.
23. Sakai D, Mochida J, Yamamoto Y, et al. Transplantation of mesenchymal stem cells embedded in atelocollagen gel to the intervertebral disc: a potential therapeutic model for disc degeneration. Biomaterials 2003;24:3531–41.
24. Sakai D, Mochida J, Iwashina T, et al. Differentiation of mesenchymal stem cells transplanted to

a rabbit degenerative disc model. Spine 2005;30: 2379–87.
25. Sakai D, Mochida J, Iwashina T, et al. Regenerative effects of transplanting mesenchymal stem cells embedded in atelocollagen to the degenerated intervertebral disc. Biomaterials 2006;27:335–45.
26. Crevensten G, Walsh AJ, Ananthakrishnan D, et al. Intervertebral disc cell therapy for regeneration: mesenchymal stem cell implantation in rat intervertebral discs. Ann Biomed Eng 2004;32:430–4.
27. Zhang YG, Guo X, Xu P, et al. Bone mesenchymal stem cells transplanted into rabbit intervertebral discs can increase proteoglycans. Clin Orthop Relat Res 2005;430:219–26.
28. Hiyama A, Mochida J, Iwashina T, et al. Transplantation of mesenchymal stem cells in a canine disc degeneration model. J Orthop Res 2008;26:589–600.
29. Leung VY, Chan D, Cheung KM. Regeneration of intervertebral disc by mesenchymal stem cells: potentials, limitations, and future direction. Eur Spine J 2006;15:S406–13.
30. Wei A, Tao H, Chung SA, et al. The fate of transplanted xenogeneic bone marrow-derived stem cells in rat intervertebral discs. J Orthop Res 2009; 3:374–9.
31. Henriksson HB, Svanvik T, Jonsson M, et al. Transplantation of human mesenchymal stems cells into intervertebral discs in a xenogeneic porcine model. Spine 2009;34(2):141–8.
32. Hoogendoorn RJ, Lu ZF, Kroeze RJ, et al. Adipose stem cells for intervertebral disc regeneration: current status and concepts for the future. J Cell Mol Med 2008;12(6A):2205–16.
33. Ganey T, Hutton WC, Moseley T, et al. Intervertebral disc repair using adipose tissue-derived stem and regenerative cells: experiments in a canine model. Spine 2009;34(21):2297–304.
34. Yoshikawa T, Ueda Y, Miyazaki K, et al. Disc regeneration therapy using marrow mesenchymal cell transplantation: a report of two case studies. Spine 2010;35(11):E475–80.
35. Carragee EJ, Hurwitz EL, Weiner BK. A critical review of recombinant human bone morphogenetic protein-2 trials in spinal surgery: emerging safety concerns and lessons learned. Spine J 2011;11:471–91.
36. Vadalà G, Sowa G, Hubert M, et al. Mesenchymal stem cells injection in degenerated intervertebral disc: cell leakage may induce osteophyte formation. J Tissue Eng Regen Med 2011. [Epub ahead of print].

ARTICLE
Journal of Cellular Biochemistry 112:2974–2986 (2011)

Journal of Cellular Biochemistry

Effects of a Glycogen Synthase Kinase-3β Inhibitor (LiCl) on c-myc Protein in Intervertebral Disc Cells

Akihiko Hiyama,[1,2]* Daisuke Sakai,[1,2] Fumiyuki Arai,[1,2] Daisuke Nakajima,[1,2] Katsuya Yokoyama,[1,2] and Joji Mochida[1,2]

[1]*Department of Orthopaedic Surgery, Surgical Science, Tokai University School of Medicine, 143 Shimokasuya, Isehara, Kanagawa 259-1193, Japan*

[2]*Research Center for Regenerative Medicine, Tokai University School of Medicine, 143 Shimokasuya, Isehara, Kanagawa 259-1193, Japan*

ABSTRACT

Wnt/β-catenin (hereafter called Wnt) signaling is a key inducer and regulator of joint development, and is involved in the formation of bone and cartilage. We previously reported that Wnt signaling plays an essential role in the control of cell proliferation and cell senescence in intervertebral disc cells. In the present study, we provide evidence that the expression of c-myc, a key protein required for cell proliferation, is regulated by Wnt signaling. Our data also show that activation of Wnt signaling by LiCl, a Wnt signaling activator, leads to the suppression of c-myc promoter activity and expression. To ascertain whether Wnt signaling regulates the expression of c-myc, we measured both its transcript and protein expression. Following treatment with LiCl, c-myc expression was suppressed at both the mRNA and protein levels. In nucleus pulposus cells treated with c-myc, cell viability increased significantly, whereas treatment with a c-myc inhibitor decreased cell viability. Taken together, these results suggest that c-myc is an important factor that promotes the proliferation of nucleus pulposus cells. These findings provide new insight into the regulation and maintenance of cell proliferation in nucleus pulposus cells. J. Cell. Biochem. 112: 2974–2986, 2011.

KEY WORDS: NUCLEUS PULPOSUS; INTERVERTEBRAL DISC DEGENERATION; WNT SIGNALING; C-MYC; CELL PROLIFERATION

The control of notochordal cell differentiation and hypertrophy plays a pivotal role in intervertebral disc degeneration. A number of signaling pathways have been implicated in the regulation of notochordal cell differentiation and hypertrophy; these include bone morphogenetic protein, transforming growth factor-β, and Wnt/β-catenin (hereafter called Wnt) signaling. Wnt signaling is a key inducer and regulator of joint development, and is involved in the formation of bone and cartilage [Cadigan and Nusse, 1997; Logan and Nusse, 2004]. Dysregulation of members of this pathway has been described in osteoarthritis [Zhu et al., 2009]. This makes the Wnt-family of proteins and signaling an attractive target for the treatment of arthritis and other joint-related diseases [Weng et al., 2010]. Glycogen synthase kinase-3β (GSK-3β) may be a particularly good target for therapeutic agents because it is an essential component of the pathway and because activation of this kinase results in the inhibition of Wnt signaling. In cells lacking the Wnt signal (off state), GSK-3β phosphorylates β-catenin, inducing rapid degradation of β-catenin via ubiquitin/proteasome signaling. In the presence of Wnt ligands (on state), activation of Wnt/β-catenin signaling is characterized by (1) stabilization of cytoplasmic β-catenin after receptor engagement by Wnt ligands; (2) β-catenin nuclear translocation; (3) β-catenin interaction with lymphoid enhancer-binding factor 1/T cell factor 1 (LEF-1/TCF-1) transcription factors; and (4) stimulation of target gene proteins such as c-myc and cyclin D1 [Behrens et al., 1996, 1998; Clevers et al., 1997; Korinek et al., 1997; Reya and Clevers, 2005; Kikuchi et al., 2006].

Regenerative therapies for intervertebral disc degeneration have been reported recently [Hiyama et al., 2007, 2008; Watanabe et al.,

Abbreviations used: GSK-3β, glycogen synthase kinase-3β; TCF/LEF, T cell factor/lymphoid enhancer factor; DKK-1, Dickkopf-1; PG, proteoglycan; BIO, 6-bromoindirubin-3′-oxime.

Additional Supporting Information may be found in the online version of this article.

Grant sponsor: The Japan Orthopaedics and Traumatology Foundation; Grant number: 0120; Grant sponsor: Ministry of Education, Culture, Sports, Science, and Technology of Japan.

*Correspondence to: Akihiko Hiyama, MD, PhD, Department of Orthopaedic Surgery, Surgical Science, Tokai University School of Medicine, Shimokasuya, Isehara, Kanagawa 259-1193, Japan. E-mail: a.hiyama@tokai-u.jp

Received 29 May 2011; Accepted 1 June 2011 • DOI 10.1002/jcb.23217 • © 2011 Wiley-Liss, Inc.
Published online 15 June 2011 in Wiley Online Library (wileyonlinelibrary.com).

2010]; however, the pathophysiology of intervertebral disc degeneration, which is thought to cause low back pain, has yet to be clearly delineated. To clarify the mechanism responsible for low back pain, it is necessary to understand the molecular mechanisms involved in intervertebral disc degeneration.

We previously analyzed Wnt signaling in nucleus pulposus cells and reported that activation of Wnt signaling suppresses the proliferation of nucleus pulposus cells and induces cell senescence [Hiyama et al., 2010], suggesting that Wnt signaling triggers the process of degeneration of the intervertebral disc. We suggested that c-myc and cyclin D1, target genes of Wnt signaling, are involved in this process [Hiyama et al., 2011]. Of these two, c-myc, a target gene of Wnt signaling, has a variety of functions involved in cell proliferation, differentiation, oncogenesis, and apoptosis [Amati and Land, 1994; Hueber et al., 1997; Schreiber-Agus and DePinho, 1998; Zindy et al., 1998]. However, despite its various functions, there are no detailed reports on the expression of c-myc and the mechanism underlying its regulation in nucleus pulposus cells. The present study was undertaken to explore whether Wnt signaling accelerates the degeneration of nucleus pulposus cells, and if so, to define the mechanism underlying this signaling. We conducted a new analysis of the expression and regulation of c-myc attributable to the activation of Wnt signaling by inhibiting GSK-3β in nucleus pulposus cells. We herein report for the first time that c-myc is an important factor that promotes the proliferation of and regulates the matrix synthesis by nucleus pulposus cells. These findings provide new insights into the regulation and maintenance of cell proliferation and matrix synthesis in nucleus pulposus cells.

MATERIALS AND METHODS

REAGENTS AND PLASMIDS

To study Wnt/β-catenin-Tcf-1/Lef-1 transcriptional activity, nucleus pulposus cells were transiently transfected with a luciferase-based Topflash (TCF optimal promoter) Wnt reporter plasmid (Millipore, Billerica, MA) or Fopflash (mutated TCF binding site promoter) reporter plasmid (Millipore). The c-myc reporter constructs (c-myc-Del1:16601, c-myc-Del2:16602, c-myc-Del3:16603, c-myc-Del4:16604, and pCX-c-myc:19772) and HA-GSK-3β wt (14753) were purchased from Addgene (Cambridge, MA). For the c-myc constructs [He et al., 1998], Tcf/Lef-binding motifs within the c-myc promoter were analyzed using a web-based tool for predicting transcription factor binding sites in DNA sequences, TESS (http://www.cbil.upenn.edu/cgi-bin/tess/tess). The plasmid for Wnt3a (sc-305570) and the backbone plasmid (pCMV6XL5) were provided by OriGene (Rockville, MD). The luciferase reporter plasmid encoding the aggrecan promoter (Agg-luc) was provided by Dr. Michael C. Naski (University of Texas Health Science Center at San Antonio). The aggrecan promoter carries 1.2 kb of the proximal mouse promoter [Reinhold et al., 2006]. As an internal transfection control, we used the empty vector pGL4.74 (Promega, Madison, WI) containing *Renilla reniformis* luciferase genes. The amount of transfected plasmid, the pre-transfection period after seeding, and the posttransfection period before harvesting were optimized for rat nucleus pulposus cells using the pSVβ-galactosidase plasmid (Promega).

To examine the intracellular mechanism of Wnt-induced β-catenin translocation, lithium chloride (LiCl) was used to inhibit the activity of GSK-3β to mimic the inhibitory effects of Dvl following activation of FZD by Wnt. At least 30 small-molecule GSK-3 inhibitors have been developed [Alonso and Martinez, 2004; Meijer et al., 2004]. Among these, LiCl is used widely for research purposes. Several groups have used the GSK-3β inhibitor LiCl to examine the relationships between Wnt signaling molecules [Stambolic et al., 1996; Spencer et al., 2006]. LiCl inhibits GSK-3β via two distinct mechanisms: by competing with Mg^{2+}, an essential cofactor for GSK-3β enzyme and by increasing the inhibitory phosphorylation of GSK-3β. Inhibition of GSK-3β leads to the accumulation of β-catenin and the activation of Wnt/β-catenin-dependent signals. We also used 6-bromoindirubin-3′-oxime (BIO) (361550, Calbiochem) to examine the activity of Wnt signaling.

Cells were also treated with recombinant Dickkopf-1 (DKK-1; 5439-DK, R&D Systems, Minneapolis, MN) to inhibit Wnt signaling. In the 3-(4,5-dimethylthiazol-2-yl)-2,5-diphenyltetrazolium bromide (MTT) assay, nucleus pulposus cells were treated with recombinant c-myc protein (CP-6012, Biomiga, San Diego, CA) or the c-myc inhibitor (10058-F4, (*Z*,*E*)-5-(4-ethylbenzylidine)-2-thioxothiazolidin-4-one) (475956, Calbiochem).

ISOLATION OF INTERVERTEBRAL DISC CELLS

A total of 64 (female n = 32, male n = 32) 12-week-old Sprague-Dawley rats were used for this study. There were no significant differences in the data between female and male rats. Rat nucleus pulposus cells were isolated using methods reported by Hiyama et al. [2010]. The rats were euthanized by injection of an excess of pentobarbital sodium (100 mg/kg) (Nembutal®, Abbott Laboratories). The spinal column was removed under aseptic conditions, and the lumbar intervertebral discs were separated under microscopy. The gel-like nucleus pulposus was separated from the annulus fibrosus. The obtained nucleus pulposus tissue was digested in a mixture of 0.01% trypsin and allowed to digest at 37°C for 15 min. Annulus fibrosus tissue was digested with 0.4% pronase for 1 h and with 0.025% collagenase P for 3 h. The digested tissue was passed through a cell strainer (BD Falcon) with a pore size of 100 μm and then washed twice with phosphate-buffered saline (PBS, Gibco). The isolated cells were maintained in Dulbecco's modified Eagle's medium (DMEM) (Cellgro, Manassas, VA) and 10% fetal bovine serum (FBS) supplemented with antibiotics in a humidified atmosphere of 5% CO_2 at 37°C. When confluent, the nucleus pulposus and annulus fibrosus cells were harvested and subcultured in 10-cm dishes. The nucleus pulposus cells have been reported to comprise at least two major cell populations, notochordal cells and chondrocyte-like cells [Trout et al., 1982]. Because cells obtained from the rat intervertebral disc tissues were variable in morphology until passages 2–3, we used low-passage (<3) cells cultured in monolayers for all experiments.

IMMUNOFLUORESCENCE STAINING

Nucleus pulposus cells were plated in flat-bottom 96-well plates (5×10^3 cells per well) and treated with LiCl (20 mM) or c-myc (100 ng/ml) for 24 h. Following treatment, the medium was

removed, cells were fixed with 4% paraformaldehyde, permeabilized with 0.2% Triton X-100 (v/v) in PBS for 10 min, and blocked with PBS containing 5% FBS. Excess serum was removed and the cells were incubated overnight at 4°C with antibodies to β-catenin (9562, 1:200 dilution, Cell Signaling, MA), c-myc (ab39688, 1:200 dilution, Abcam, Cambridge, UK), and aggrecan (MA3-16888, 1:200 dilution, Thermo Scientific, Fremont, CA). After washing, cells were incubated with an anti-rabbit IgG Alexa Fluor 488 (green) and 594 (red) secondary antibodies (Invitrogen, Camarillo, CA), each at a dilution of 1:50, and 10 μm DAPI, for 1 h at room temperature for nuclear staining. Microscopic analyses were performed with a fluorescence microscope connected to a digital imaging system.

IMMUNOHISTOLOGICAL STUDIES

For immunohistochemistry, freshly isolated spinal tissues from 3- to 12-week-old rats were fixed immediately in 4% paraformaldehyde in PBS and embedded in paraffin. Transverse and coronal sections were deparaffinized in xylene, rehydrated through a graded ethanol series, and stained with hematoxylin and eosin. To localize c-myc, sections were incubated with the anti-c-myc antibody (ab39688, Abcam) in 2% bovine serum albumin (BSA) in PBS at a dilution of 1:200 at 4°C overnight. After thorough washing of the sections, to detect the bound primary antibody the sections were incubated with a biotinylated universal secondary antibody at a dilution of 1:20 (Vector Laboratories, Burlingame, CA) for 10 min at room temperature. The sections were then incubated with a streptavidin/peroxidase complex for 5 min and washed with PBS, and the color was developed using 3′-3-diaminobenzidine (Vector Stain Universal Quick Kit, Vector Laboratories).

MTT ASSAY

The effect of the treatments on cell proliferation was also measured by a modified MTT assay, based on the ability of live cells to utilize thiazolyl blue and convert it into the water-insoluble dark-blue formazan stain. Exponentially growing nucleus pulposus cells were seeded in 24-well plates at 1.5×10^4 cells per well. The cells were allowed to adhere for 24 h in DMEM containing 2% FBS, and the medium was replaced with DMEM containing 0.5% FBS. Cells were stimulated with LiCl (20 mM), c-myc (100 ng/ml), or c-myc inhibitor (20 μM) for 24 h, and the cells were then treated with MTT (5 g/L; Sigma) for 2 h at 37°C. Dimethyl sulfoxide (DMSO) was added to each well, the reaction was incubated for 30 min, and the cells were transferred to a 96-well plate. A 96-well microtiter plate reader (Pharmacia) was used to quantify the *A*590. After c-myc and c-myc inhibitor stimulation, nucleus pulposus cells were also treated with MTT. All experiments were performed three independent times in triplicate.

CELL-CYCLE ANALYSIS BY FLUORESCENCE-ACTIVATED CELL SORTING (FACS)

Nucleus pulposus cells were grown at a seeding density of 5×10^4 cells/ml in 24-well plates under a humidified 5% CO_2 atmosphere at 37°C. The cells were allowed to adhere for 24 h in medium containing 2% FBS. The culture medium of each flask was then replaced with medium containing 0.5% FBS. c-myc (100 ng/ml) was added to this medium as a concentrated stock solution dissolved in DMSO, and the cells were incubated for an additional 24 h. The cell-cycle distribution of the nucleus pulposus cells was analyzed by flow cytometry after DNA staining with propidium iodide using the CycleTEST™ PLUS kit (BD PharMingen, San Diego, CA). CELLQuest (BD PharMingen) and ModiFit LT (BD PharMingen) software packages were used for cell acquisition and analysis. Each experiment was performed in duplicate, and the results from three individual experiments are shown.

REAL-TIME RT-PCR ANALYSIS

The nucleus pulposus cells and annulus fibrosus cells were cultured in 6-cm plates (5×10^5 cells per plate) with or without 20 mM LiCl, and total RNA was extracted using the TRIzol RNA isolation protocol (Invitrogen). The total RNA of nucleus pulposus tissues and annulus fibrosus tissues was also extracted. Before elution from the column, RNA was treated with RNase-free DNase I. The total RNA (100 ng) was used as a template for the real-time PCR analyses. The mRNA was quantified using the ABI 7500 Fast Real-Time PCR System (Applied Biosystems, Foster City, CA), and cDNA was synthesized by the reverse transcription of mRNA as described previously [Hiyama et al., 2010]. The real-time PCR analyses were performed in 96-well plates with the Fast SYBR Green Master Mix (Applied Biosystems). PCR reactions were performed in a StepOnePlus real-time PCR system (Applied Biosystems). Two microliters of cDNA per sample was used as the template for real-time PCR: 1 μl forward primer and 1 μl reverse primer were added to 20 μl of SYBR Green Master Mix. The reactions were synthesized in a 20-μl reaction volume under the following conditions: an initial step at 50°C for 2 min, followed by 95°C for 10 min, and 40 cycles at 95°C for 3 s (denaturation) and 30 s at 60°C (hybridization/elongation). All primers (β-catenin, c-myc, GSK-3β, and aggrecan) were synthesized by Takara Bio, Inc. (Tokyo, Japan): β-catenin (NCBI number: AF_121265.1) forward, 5′-GCCAGTGGATTCCGTACTGT-3′ and reverse, 5′-GAGCTTGCTTTCC-TGATTGC-3′; c-myc (NCBI number: NM_012603.2) forward, 5′-AATCCTGTACCTCGTCCGATTCC-3′ and reverse 5′-TTTCCACAGA-CACCACATCAATTTC-3′; GSK-3β (NCBI number: NM_032080.1) forward, 5′-GTCAAACTACCAAATGGGCGAGA-3′ and reverse, 5′-GCCAGAGGTGGGTTACTTGACAG-3′; and aggrecan (NCBI number: NM_022190.1) forward, 5′-TCCGCTGGTCTGATGGACAC-3′ and reverse, 5′-CCAGATCATCACTACGCAGTCCTC-3′. To normalize each sample, a control gene (GAPDH) was used, and the arbitrary intensity threshold (C_t) of amplification was computed. The expression scores were obtained by the $\Delta\Delta C_t$ calculation method. The relative amounts of mRNA were calculated using the software program Microsoft Excel.

WESTERN BLOTTING ANALYSIS

To detect β-catenin, the nucleus pulposus cells were cultured with or without 20 mM LiCl for 24 h. To detect total c-myc and phosphorylated c-myc, the nucleus pulposus cells were stimulated with LiCl (20 mM) for 6–24 h. Immediately after treatment, the nucleus pulposus cells were placed on ice and washed with cold PBS. Proteins were prepared using the CelLytic NuCLEAR extraction kit (Sigma–Aldrich). All wash buffers and the final resuspension buffer included 1× protease inhibitor cocktail (Pierce, Thermo Scientific, Rockford, IL), NaF (5 mM), and Na_3VO_4 (200 mM). Nuclear or total

cell proteins were resolved on sodium dodecyl sulfate (SDS)-polyacrylamide gels and were electrotransferred to nitrocellulose membranes (Bio-Rad). The membranes were blocked with 5% BSA in TBST (50 mM Tris, pH 7.6, 150 mM NaCl, and 0.1% Tween-20) and were incubated overnight at 4°C in 5% BSA in TBST. Antibodies to β-catenin (9562, 1:1,000 dilution, Cell Signaling) and c-myc (ab39688, 1:1,000 dilution, Abcam) were used as the primary antibodies. β-Actin was used as an internal control. The ECL detection system (Amersham Biosciences, GE Healthcare, Eindhoven, the Netherlands) was used to detect the specific signals.

TRANSFECTIONS AND DUAL LUCIFERASE ASSAY

Nucleus pulposus cells were transferred to 24-well plates at a density of 6×10^4 cells per well 1 day before transfection. The next day, nucleus pulposus cells were treated with 1, 10, or 20 mM LiCl with 900 ng of Topflash reporter plasmid and 100 ng of the pGL4.74 plasmid for 8–24 h. We also performed the same experiments using BIO. In several experiments, cells were cotransfected with 100–500 ng of GSK-3β wt, Wnt3a, or an appropriate backbone vector with 400 ng of c-myc deletion reporters and 100 ng of the pGL4.74 plasmid. Lipofectamine 2000 (Invitrogen) was used as the transfection reagent. For each transfection, plasmids were premixed with the transfection reagent. After 24 h, the cells were harvested, and a dual-luciferase reporter assay system (Promega) was used for the sequential measurements of *firefly* and *Renilla* luciferase activities. The results were normalized for transfection efficiency and are expressed as a relative ratio of luciferase to pGL4.74 activities (denoted as relative activity). To check the transfection efficiency, nucleus pulposus cells were transfected with plasmid encoding GFP. In several experiments, a construct of GFP was used as the negative control. The transfection efficiency for nucleus pulposus cells was about 60–70%. Luciferase activities were quantified and relative ratios were calculated using a Turner Designs Luminometer Model TD-20/20 instrument (Promega). At least three independent transfections were performed, and all analyses were performed in triplicate.

STATISTICAL ANALYSIS

All measurements were performed in triplicate. Statistical significance was analyzed using the SPSS14.0 software program and Kruskal–Wallis nonparametric analysis and Mann–Whitney *U* post hoc testing. Results are presented as the mean ± SEM. Differences between groups were assessed by analysis of variance. *P*-values <0.05 were considered statistically significant.

RESULTS

PROMOTION AND REGULATION OF WNT/β-CATENIN ACTIVITY IN NUCLEUS PULPOSUS CELLS

To determine the role of Wnt signaling in nucleus pulposus cells, we first evaluated Wnt signal activation by examining the β-catenin protein levels in nucleus pulposus cells from 12-week-old rats. As shown in Figure 1A, immunoblotting analysis and densitometry of nucleus pulposus cells showed that the level of total β-catenin was higher in LiCl-treated cells compared with control nucleus pulposus cells. By contrast, LiCl treatment decreased the level of phospho-β-

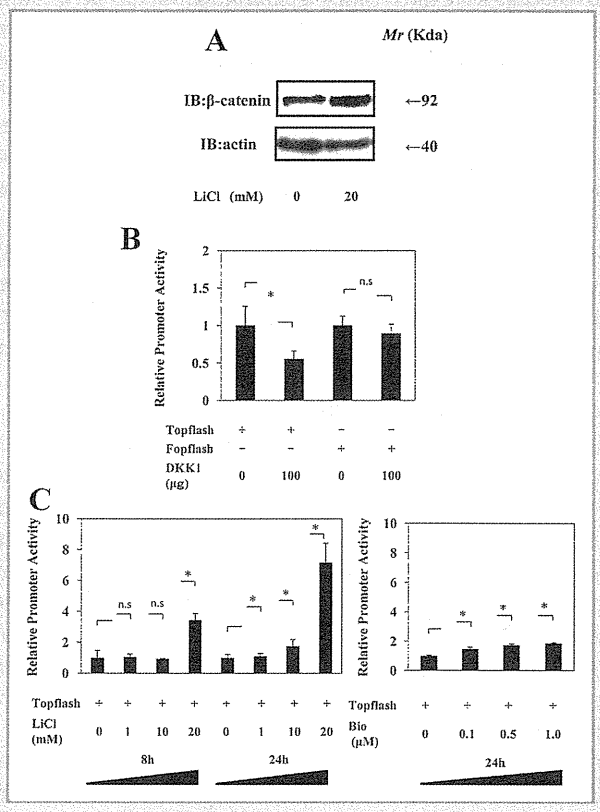

Fig. 1. Regulation of Wnt/β-catenin activity in nucleus pulposus cells. A: Western blot analysis showed increased detectable β-catenin protein levels after treatment with LiCl. B: Cells transfected with the Topflash reporter plasmid or Fopflash along with the pGL4.74 plasmid were cultured with or without DKK-1 (0.1 μg/ml), and the reporter activity was measured. C: Cells transfected with the Topflash reporter plasmid and the pGL4.74 plasmid were treated with different concentrations of LiCl (left panel) or BIO (right panel), and the reporter activity was measured. Values are expressed as the mean ± SD. $^*P < 0.05$. n.s., not significant.

catenin (data not shown). To confirm whether Dkk-1, a secretory protein that inhibits Wnt signaling by disrupting the interactions between Wnt and Fz, suppresses the transcriptional activity of Topflash, we assessed the transcriptional activity of Topflash or Fopflash following the addition of DKK-1 (0.1 μg/ml) for 24 h. The activity of Topflash decreased after DKK-1 stimulation, and as expected, the Fopflash promoter activity was unresponsive to DKK-1 stimulation (Fig. 1B).

Next, to confirm the activation or suppression of Wnt signaling in nucleus pulposus cells, we examined whether Wnt signaling is promoted by different concentrations and durations of treatment with the Wnt activators LiCl or BIO in nucleus pulposus cells. Our previous study showed that LiCl treatment (20 mM, 24 h) upregulated β-catenin signaling eightfold in Topflash-transfected cultures but not in Fopflash-transfected cultures [Hiyama et al., 2010]. However, there are no detailed reports on the activation of Wnt signaling by LiCl and BIO in nucleus pulposus cells. Nucleus pulposus cells were transfected with Topflash and treated for different times and at different concentrations of LiCl or BIO. After

8–24 h, we measured the activity of Topflash in nucleus pulposus cells. Figure 1C shows that there was a dose- and time-dependent increase in the activity of Topflash with LiCl or BIO stimulation. Inhibition of GSK-3β with LiCl or BIO stimulated Topflash transcription in nucleus pulposus cells compared with that in untreated cells.

It is interesting that the level of Topflash activity was considerably higher after treatment with LiCl than after treatment with BIO. We thought that the LiCl concentration may have been higher than the BIO concentration. However, Mazumdar et al. [2010] reported that LiCl (20 mM) and BIO (200 nM) activate Wnt. Therefore, we believed that activation of Wnt signaling in nucleus pulposus cells has a higher affinity for stimulation by LiCl than by BIO. We also examined the gene expression levels of Wnt proteins following treatment with LiCl (20 mM, 24 h). Real-time PCR arrays showed that treatment with LiCl upregulated gene expression of *Wnt1*, *Wnt4*, *Wnt6*, and *Wnt16* compared with that of untreated control cells; gene expression of *Wnt3a*, *Wnt5a*, *Wnt5b*, and *Wnt10a* was not upregulated (Supplemental Fig. 1A).

PROMOTION AND REGULATION OF C-MYC BY WNT SIGNALING IN NUCLEUS PULPOSUS CELLS

We also investigated the mechanism underlying the c-myc regulation by LiCl using Western blot analysis to determine the effects of mimicking Wnt signaling on the expression of c-myc protein in nucleus pulposus cells. Treating the cells with LiCl at 20 mM for 6–24 h produced the best results. For c-myc, two bands were detected: the upper band (65 kDa) was the phosphorylated form of c-myc protein and the lower band (49 kDa) was the unphosphorylated form. These results demonstrated that LiCl treatment led to a time-dependent decrease in c-myc protein expression in nucleus pulposus cells and that the decrease was most pronounced 24 h after treatment (Fig. 2A). To verify the Western blotting data, we next performed real-time PCR analysis of c-myc mRNA expression following treatment with LiCl (20 mM, 24 h). Figure 2B shows that treatment with LiCl for 24 h decreased c-myc mRNA levels. We also measured the expression level of several genes in intervertebral disc tissues, including c-myc and GSK-3β. Interestingly, both c-myc and GSK-3β gene expression was much higher in nucleus pulposus tissues than in annulus fibrosus tissues (Fig. 2C). This suggests that

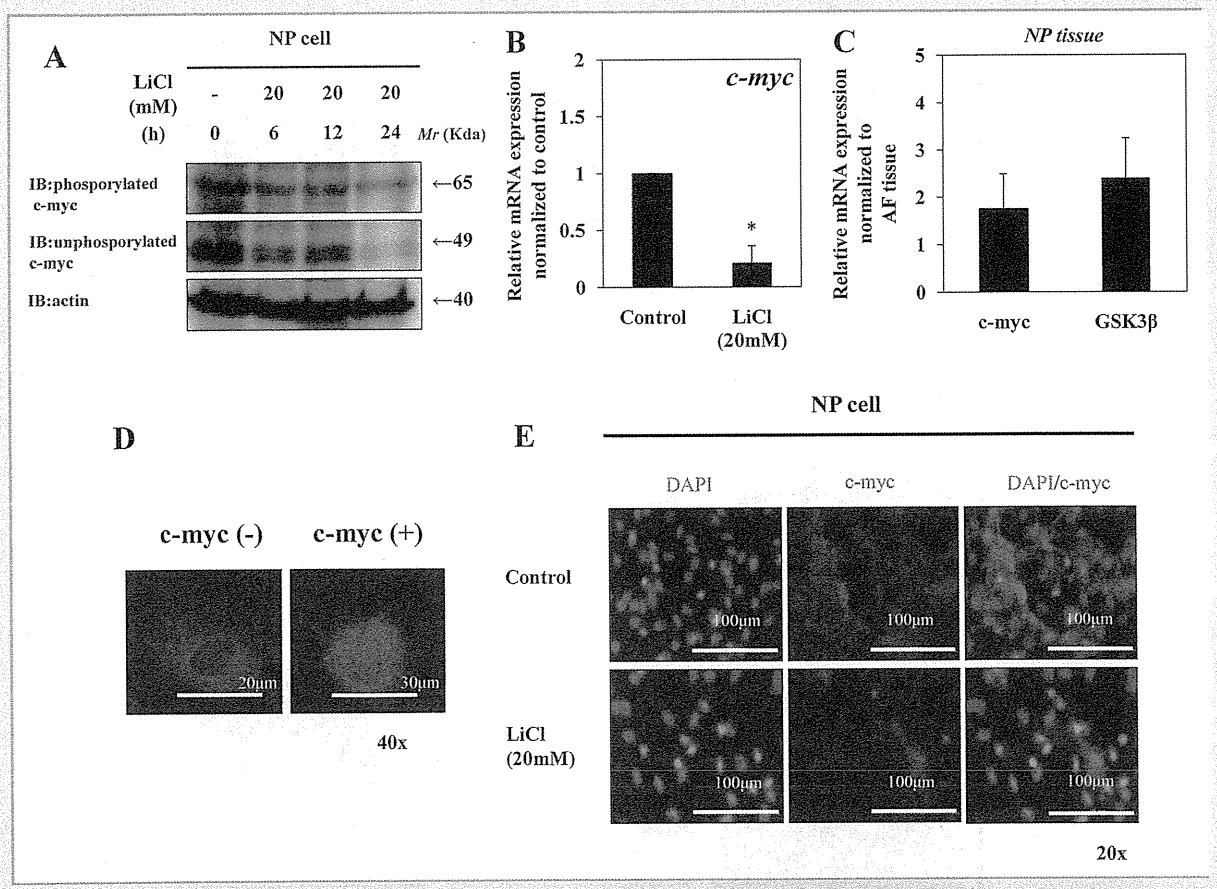

Fig. 2. Regulation of c-myc by Wnt signaling in nucleus pulposus cells. A: Western blot analysis using an anti-c-myc antibody demonstrated that LiCl treatment decreased c-myc protein expression in nucleus pulposus cells 6–24 h after treatment with 20 mM LiCl. B: Real-time RT-PCR analysis of c-myc mRNA levels in nucleus pulposus cells cultured for 24 h in the presence or absence of 20 mM LiCl. Values are expressed as the mean ± SD. $^{*}P < 0.05$. C: We examined the relative c-myc and GSK3β mRNA expression in nucleus pulposus tissue normalized to that of annulus fibrosus tissue. D: The expression of c-myc after treatment of recombinant c-myc protein was assessed in nucleus pulposus cells by immunofluorescence analysis. Bars indicate 20–30 μm; original magnification 40×. E: Nucleus pulposus cells were grown in 96-well plates and exposed to LiCl (20 mM) for 24 h. Representative results of immunocytochemistry using anti-c-myc (red) and DAPI (blue) are shown. The results are representatives of three independent experiments per protein. Bars indicate 20–100 μm; original magnification 20×.

the c-myc and GSK-3β genes may be more important in nucleus pulposus cells than in annulus fibrosus cells.

To determine whether recombinant c-myc protein led to activation of c-myc-dependent transcription, we performed immunofluorescence analysis. The immunofluorescence analysis indicated that there was a concomitant increase in c-myc protein expression in nucleus pulposus cells treated with exogenous c-myc at 100 ng/ml for 24 h. The c-myc treatment induced total c-myc levels and promoted the nuclear translocation of c-myc more strongly in nucleus pulposus cells than in untreated cells. We also observed detectable amounts of c-myc in the cytoplasm (Fig. 2D). Immunofluorescence analysis also showed a concomitant decrease in c-myc protein expression in nucleus pulposus cells treated with LiCl at 20 mM for 24 h (Fig. 2E).

EXPRESSION OF C-MYC PROTEIN IN THE INTERVERTEBRAL DISC IN VIVO

We examined whether there is expression of c-myc protein in the intervertebral disc tissues. We performed immunostaining of saggital sections from 12- to 3-week-old rats with an antibody to c-myc, or counterstained the sections with hematoxylin for morphology assessment. We found that c-myc is expressed by cells of the nucleus pulposus (A–C) and annulus fibrosus (D–F) in the 12-week-old rat disc, whereas the expression of c-myc level of 3-week-old rat disc (G–I) was higher than that of 12-week-old rat. In all cases, much more of the staining was localized to the nucleus than the cytosol and plasma membrane (Fig. 3).

C-MYC REGULATES CELL VIABILITY IN NUCLEUS PULPOSUS CELLS

To test whether Wnt signaling activation is sufficient to promote or inhibit nucleus pulposus cell proliferation, the viability of cells was evaluated using the MTT assay. The number of viable cells decreased by 30% following LiCl treatment (Fig. 4A). Wnt3a treatment was sufficient to inhibit nucleus pulposus cell proliferation (data not shown). We also examined whether nucleus pulposus cell proliferation is regulated by c-myc. Treatment of nucleus pulposus cells with c-myc (100 ng/ml) significantly increased viability (Fig. 4B). To examine whether increased c-myc activity promotes cell proliferation in nucleus pulposus cells, we inhibited c-myc activity with 10058-F4, a small-molecule c-myc inhibitor known to

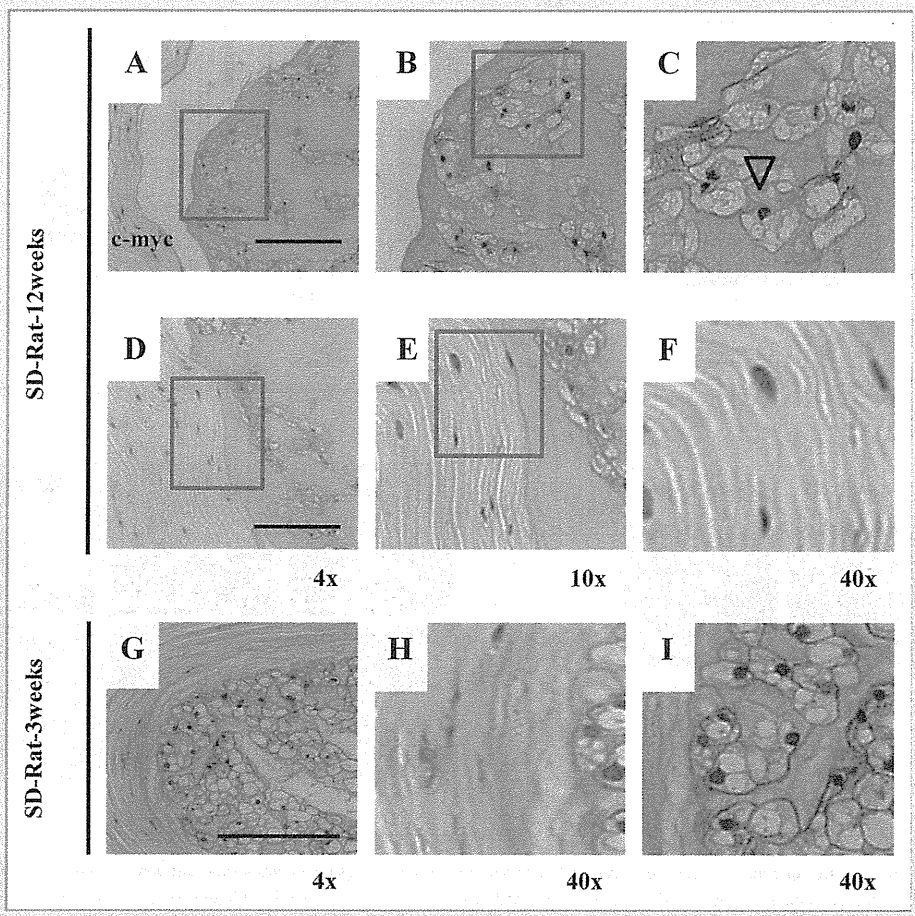

Fig. 3. Sagittal sections of an intervertebral disc from a Sprague–Dawley rat (12 and 3 weeks of age). The boxed area in the left panel (4×) is shown at higher magnification in the right panel (40×). The c-myc level in the nucleus pulposus (A–C) and annulus fibrosus (D–F) cells in the 12-week-rat disc, whereas the c-myc level was detected in 3-week-rat disc (G–I) both annulus fibrosus (H) and nucleus pulposus (I) (40×). Note that the nucleus pulposus cells and annulus fibrosus cells both express the c-myc protein (arrows in C, F, H, and I). Bars are 100–200 μm.

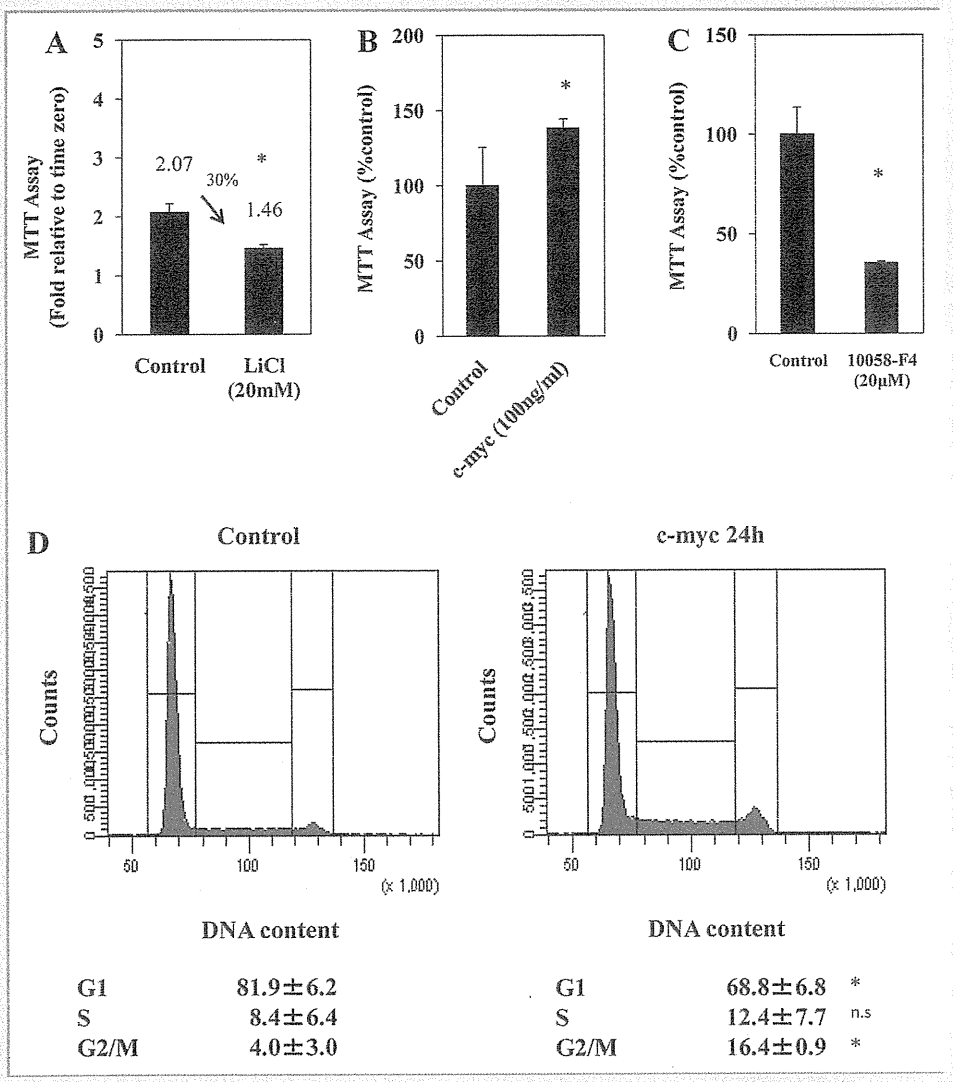

Fig. 4. Measurement of cell viability in nucleus pulposus cells. A: Nucleus pulposus cells were pretreated for 24 h with 20 mM of LiCl, and cell viability was determined by the MTT assay. B,C: Cell viability after treatment with c-myc (B) or the c-myc inhibitor 10058-F4 (C) was measured using the MTT assay. D: Nucleus pulposus cells were cultured for 24 h, and the cells were treated with or without c-myc (100 ng/ml) for 24 h and harvested, and the nuclei were stained with propidium iodide. DNA histograms were generated using flow cytometry. Each plot represents the analysis of 10,000 events. The histograms present typical results, and the percentages of cells in G1, S, and G2/M cell-cycle phases are shown as the means of triplicate measurements. Values are expressed as the mean ± SD. $^{*}P < 0.05$. n.s., not significant.

inhibit heterodimerization between c-myc and max, preventing c-myc from transactivating its transcriptional target genes [Yin et al., 2003; Huang et al., 2006]. The nucleus pulposus cells were treated with 10058-F4 (20 μM) for 24 h, and cell viability was measured using the MTT assay. Treatment with 10058-F4 decreased cell viability (Fig. 4C). Together, these results suggest that c-myc is an important factor that promotes the proliferation of nucleus pulposus cells.

We then used flow cytometry to study cell-cycle progression by quantifying DNA and the effects of activation of c-myc. After serum deprivation, 81.9 ± 6.2% of the nucleus pulposus cells were in the G1 phase, 8.4 ± 6.4% in the S phase, and 4.0 ± 3.0% in the G2/M phase. Treatment with c-myc (100 ng/ml) for 24 h significantly decreased the percentage of cells in the G1 phase to 68.8 ± 6.8% and increased the percentage of cells in the S phase and G2/M phase to 12.4 ± 7.7% and 16.4 ± 0.9%, respectively (Fig. 4D).

EFFECT OF THE C-MYC PROMOTER ON THE WNT SIGNALING IN NUCLEUS PULPOSUS CELLS

We further investigated the regulation of c-myc expression by analyzing the 2.26-kb promoter sequence of human c-myc and measuring the activity of different-sized promoter constructs (Fig. 5A). The c-myc promoter contains 14 Tcf/Lef-binding motifs: 13 Tcf/Lef-binding motifs in the p-c-myc-Del1 construct and three Tcf/Lef-binding motifs in the p-c-myc-Del4 construct. To analyze the promoter function further, we used luciferase reporter constructs containing a −2,263/+513 bp (p-c-myc-Del1), −1,055/+513 bp (p-c-myc-Del2), −605/+513 bp (p-c-myc-Del3), or −348/

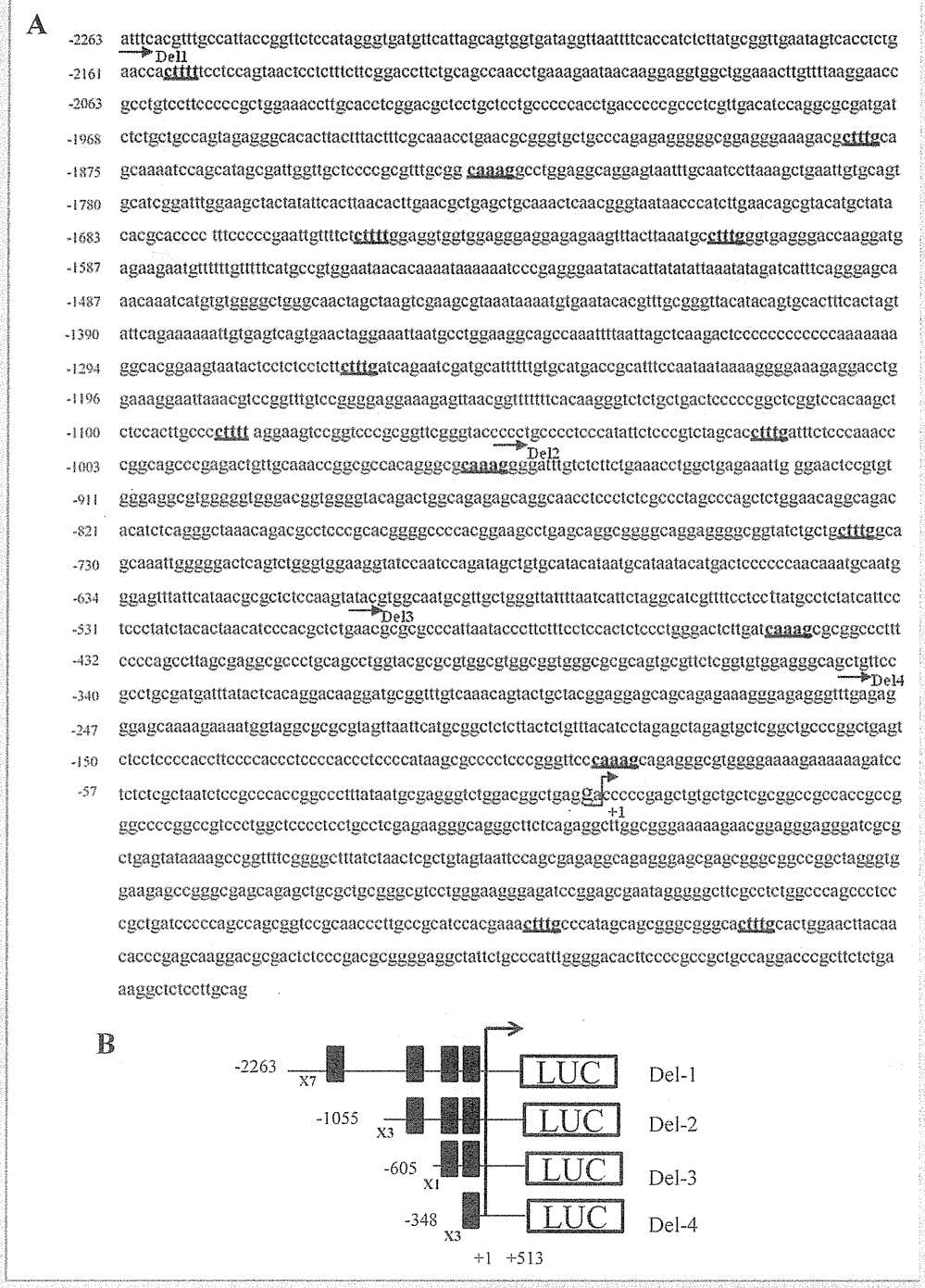

Fig. 5. Tcf- and Lef-binding motifs contained in the c-myc promoter. A: The DNA sequence of the promoter region of the c-myc gene [He et al., 1998]. Tcf/Lef (CTTTT, CTTTG, or CAAAG) consensus sequences are marked in boldface type and underlined. The arrows indicate the starting location of the primers used to generate the promoter constructs. The transcription start site is marked as +1; GAC marks the translation start site. B: The transcription start site is marked as +1. The Tcf/Lef-binding motifs are shown as rectangles. The p-c-myc-Del1 construct comprised a 2,776-bp fragment containing 2,263 bp of the upstream c-myc promoter sequence linked to 513 bp of exon 1 (i.e., −2,263/+513), whereas the p-c-myc-Del2, p-c-myc-Del3, and p-c-myc-Del4 constructs contained a 1,568-bp fragment (−1,055/+513), 1,118-bp fragment (−605/+513), and 861-bp fragment (−348/+513), respectively.

+513 bp (p-c-myc-Del4) construct of the human c-myc promoter (Fig. 5B). We measured the basal activity of all four constructs in nucleus pulposus cells. Figure 6A shows that the −348/+513-bp (p-c-myc-Del4) construct had maximal basal activity, whereas the −2,263/+513-bp (p-c-myc-Del1) construct exhibited the lowest activity.

We next examined the effect of GSK-3β on the activities of all the c-myc promoters in nucleus pulposus cells. Treatment of nucleus

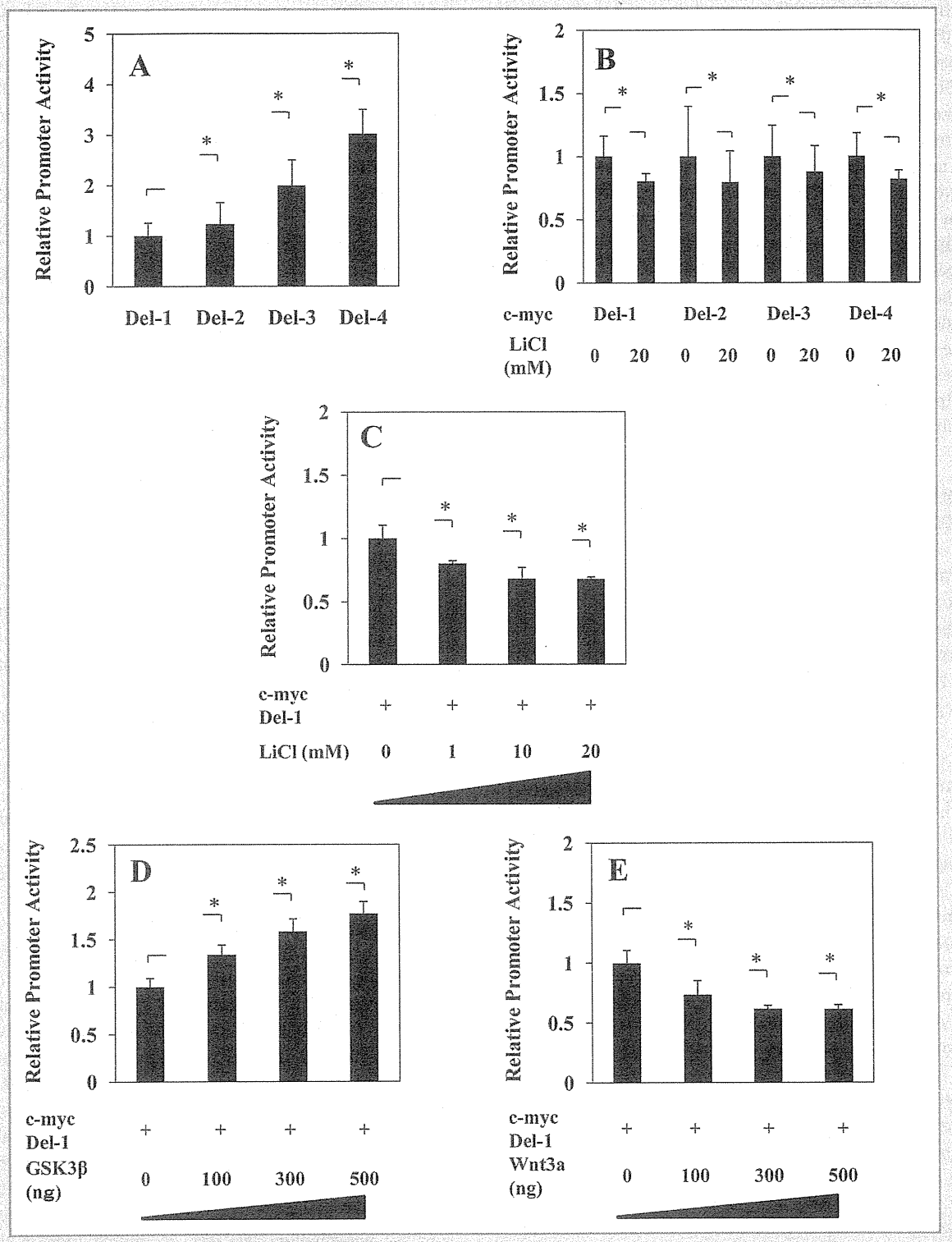

Fig. 6. Effect of c-myc reporter activity on Wnt signaling in nucleus pulposus cells. A: Basal activities of the c-myc reporter constructs in the nucleus pulposus cells were measured by a dual luciferase assay. B: The effect of LiCl on the activities of all c-myc promoters in nucleus pulposus cells. C: The cells transfected with the p-c-myc-Del1 reporter plasmid were treated with different concentrations of LiCl (1–20 mM). D: Nucleus pulposus cells were cotransfected with the p-c-myc-Del1 reporter plasmid along with WT-GSK3β or an empty vector and the pGL4.74 vector. E: Nucleus pulposus cells were cotransfected with the p-c-myc-Del1 reporter plasmid along with WT-Wnt3a or an empty vector and the pGL4.74 vector. Values are expressed as the mean ± SD. $^{*}P < 0.05$. n.s., not significant.

pulposus cells with LiCl (20 mM) decreased the activity of all c-myc promoters (Fig. 6B). To confirm these results, a p-c-myc-Del1 reporter plasmid was transfected into nucleus pulposus cells along with the pGL4.74 vector, and the cells were stimulated with LiCl. Figure 6C shows that the p-c-myc-Del1 reporter activity decreased after LiCl treatment of the nucleus pulposus cells in a dose-dependent manner. To further confirm the regulation of Wnt signaling, we examined the effect of GSK-3β (loss of function) or Wnt3a (gain of function) treatment on c-myc promoter activity in nucleus pulposus cells. Nucleus pulposus cells were transiently cotransfected with plasmids encoding GSK-3β (Fig. 6D) or Wnt3a (Fig. 6E). The p-c-myc-Del1 promoter activity was activated in a dose-dependent manner by the GSK-3β expression plasmid, whereas the p-c-myc-Del1 promoter activity was decreased by the Wnt3a expression plasmid in a dose-dependent manner in the nucleus pulposus cells. These data were opposite to the results obtained with knockdown of GSK-3β or Wnt3a (data not shown).

C-MYC REGULATES AGGRECAN ACTIVITY IN NUCLEUS PULPOSUS CELLS

The role of c-myc on aggrecan, the major structural component of intervertebral discs, is unknown. We analyzed the role of c-myc in the regulation of aggrecan. First, we assessed the effects of c-myc on aggrecan reporter (Agg-luc) activity. The cells were cultured for 48 h after transfection, and the reporter activity was measured thereafter (left panel). Nucleus pulposus cells were also cotransfected with the aggrecan reporter plasmid (Agg-luc) and pGL4.74 plasmid. The transfected cells were treated with or without a c-myc inhibitor (10058-F4) (5 μM), and the reporter activity was measured 24 h after treatment (right panel). The aggrecan reporter activity was suppressed in a c-myc concentration-dependent manner (Fig. 7A). To confirm the reporter assay data, we next performed real-time PCR analysis of aggrecan mRNA expression following treatment with c-myc (100 ng/ml, 24 h). Treatment with c-myc for 24 h significantly decreased the gene expression of aggrecan compared with that in untreated control cells (Fig. 7B). The same results were observed for aggrecan protein expression (Fig. 7C). Finally, to examine the effect of c-myc protein on Wnt signaling in nucleus pulposus cells, we used a c-myc expression plasmid in the Topflash reporter assay. Activation of c-myc significantly decreased the Topflash reporter activity in a dose-dependent manner in nucleus pulposus cells (Fig. 7D). We also performed real-time PCR analysis of β-catenin mRNA expression following treatment with c-myc (100 ng/ml, 24 h). c-myc treatment inhibited gene expression of β-catenin compared with that in untreated control cells (Supplemental Fig. 1B).

DISCUSSION

Some reports have suggested that the c-myc gene is transcribed in a strictly proliferation-dependent manner in several cell types [Mateyak et al., 1997; Morin et al., 1997; Bouchard et al., 1998]. However, the mechanism underlying the regulation of cell proliferation in nucleus pulposus cells is not well understood. The present study demonstrated for the first time that the expression of c-myc, a key protein required for cell proliferation, is regulated by Wnt signaling in nucleus pulposus cells. Our data show that activation of Wnt signaling by LiCl leads to the suppression of c-myc promoter activity and expression. We also performed deletion analysis to study the relationship between the Tcf/Lef binding sites and c-myc expression (Fig. 5). We observed that c-myc expression was regulated by Tcf/Lef binding sites in nucleus pulposus cells. We also examined the role of c-myc, including both loss of function and gain of function, in nucleus pulposus cell proliferation and cell-cycle progression. The results of the MTT assay and cell-cycle analysis showed that cell proliferation and cell-cycle progression increased 24 h following the addition of c-myc and that cell proliferation was significantly suppressed 24 h following the addition of a c-myc inhibitor.

Similar experiments using another GSK-3 inhibitor, BIO, demonstrated that the transcriptional activity of Topflash was lower and the c-myc response was weaker than when LiCl was added. The discrepancies in these effects might reflect differences in the effects of GSK-3β inhibitors in nucleus pulposus cells. GSK-3β is involved in several diverse pathways, and we cannot exclude the possibility that LiCl and BIO function via target pathways other than GSK-3β in nucleus pulposus cells. In addition, the selectivity and adequate concentration of most of the available GSK-3β inhibitors has been poorly characterized. Experimental evidence shows that certain concentrations of LiCl and/or BIO inhibit the role of GSK-3β in Wnt signaling. However, considering that LiCl increased the transcriptional activity of Topflash more than did BIO and the results of the gene expression experiments, we believe that LiCl may be a more effective activator of Wnt signaling than BIO in nucleus pulposus cells.

It was suggested originally that c-myc is a target gene of Wnt signaling and that the expression of c-myc is increased by Wnt signaling. However, in our experiments, activation of Wnt signaling by LiCl produced opposite results; that is, LiCl suppressed c-myc expression in nucleus pulposus cells via Tcf/Lef binding sites. The results of the studies described herein suggest that this mechanism may be specific to nucleus pulposus cells because the nucleus pulposus is unique both embryologically and functionally. It is also possible that LiCl induces other pathways directly. LiCl inhibits GSK-3β, causing accumulation of β-catenin, but also leads to changes in the expression of other proteins. Our previous results indicated that LiCl markedly inhibits the expression of both ERK1 and ERK2 genes, which are downstream of the TGF/BMP signal. In addition, we reported that blocking the MAPK pathway with PD98059 has an effect on the inhibition of Wnt signaling; that is, activation of Wnt signaling by the TGF/BMP signal may be regulated by Smad-independent signals [Hiyama et al., 2011]. Berridge et al. [1982] reported that LiCl inhibits inositol monophosphatase phosphatase (IMPase), decreasing inositol trisphosphate (IP3) synthesis and negatively regulating phospholipase C signaling (IP3–PLC–protein kinase C (PKC) signaling). Moreover, Madiehe et al. [1995] reported that treatment of HL60 cells with LiCl at a concentration >10 mM decreases cell proliferation and induces cell-cycle arrest because Li^+ inhibits IMPases. Building on these studies, future studies should address the role of c-myc to determine whether LiCl regulates other signals such as non-Smad pathways including MAPK, Rho-like GTPase signaling, phosphatidylinositol-3 kinase/

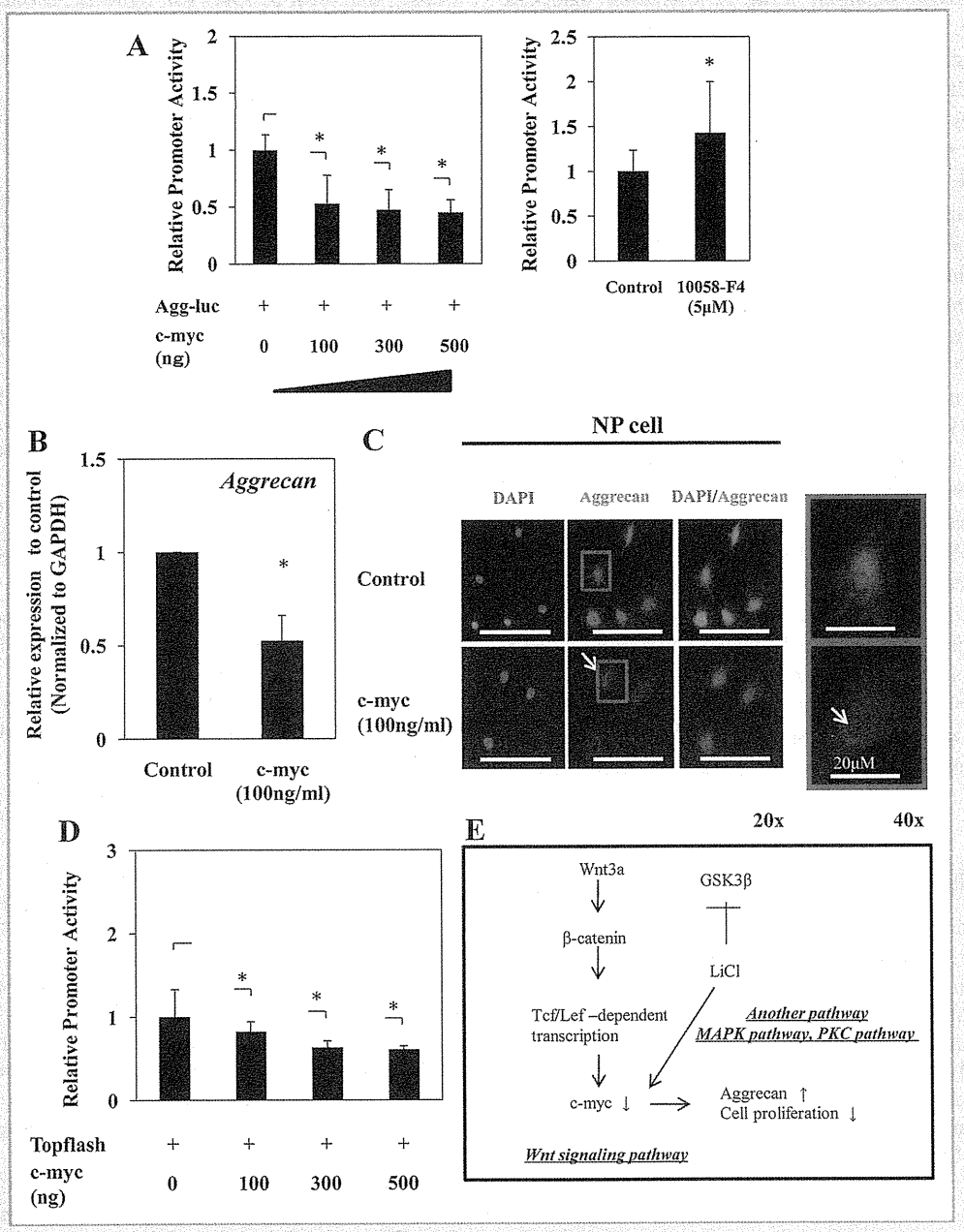

Fig. 7. Effect of aggrecan activity on the activation of c-myc in nucleus pulposus cells. A: The aggrecan reporter plasmid (Agg-luc) was transfected into nucleus pulposus cells along with a c-myc expression plasmid (left panel). The transfected cells were treated with or without a c-myc inhibitor (10058-F4) (right panel). B: Real-time RT-PCR analysis of aggrecan mRNA levels in nucleus pulposus cells cultured for 24 h in the presence or absence of c-myc. C: Nucleus pulposus cells were exposed to recombinant c-myc (100 ng/ml) for 24 h. Representative results of immunocytochemistry using anti-aggrecan (green) and DAPI (blue) are shown. Bars indicate 20–100 μm; original magnification 20–40×. D: Nucleus pulposus cells were cotransfected with the Topflash reporter plasmid along with c-myc plasmid. E: A schematic diagram of Wnt signaling in intervertebral disc cells. Values are expressed as the mean ± SD. $^{*}P < 0.05$. [Color figure can be seen in the online version of this article, available at http://wileyonlinelibrary.com/journal/jcb]

protein kinase B (PI3K/AKT), c-Jun N-terminal kinases (JNKs), and PKC.

Recent studies have suggested that Wnt signaling plays an important role in the regulation of skeletal function. In our experiments, β-catenin, an important factor for Wnt signaling, was expressed in the notochord at the developmental stages, suggesting that Wnt signaling regulates via c-myc the number of nucleus pulposus cells during the process of transformation from notochordal cells into chondrocyte-like cells. We also examined the role of c-myc and its response to factors involved in cell proliferation and its effects on aggrecan, a structural component of nucleus pulposus cells [Trout et al., 1982]. Our results suggest that c-myc significantly suppresses aggrecan expression in nucleus pulposus cells. This result is consistent with the signaling regulatory mechanism because activation of Wnt signaling by LiCl suppresses c-myc expression in nucleus pulposus cells via Tcf/Lef binding sites

and activation of Wnt signaling leads to increased aggrecan synthesis. However, it is difficult to elucidate this mechanism because there is much cross-talk between Wnt signaling and other signals. Considering the contradictory results that activation of Wnt signaling suppresses proliferation of nucleus pulposus cells but increases aggrecan synthesis, we believed that signal pathways other than the Wnt signaling are involved in intervertebral disc degeneration because of changes in aggrecan synthesis.

In summary, we showed that Wnt signaling and c-myc form a negative feedback loop in nucleus pulposus cells. However, the precise mechanism responsible for this suppression is still unclear. One limitation of using this particular inhibitor, LiCl, as a Wnt activator is that LiCl may induce cross-talk with a pathway other than Wnt signaling in vitro. The results of these experiments and our previous studies on Wnt signaling suggest one possible explanation; that the expression of β-catenin appears in the notochord in the early stages of development and that, when inactivated, Wnt signaling contributes to the maintenance of homeostasis in the intervertebral disc. Wnt signaling activation by some trigger would activate c-myc and induce intervertebral disc cell senescence, which would stop cell proliferation and ultimately cause degeneration of the intervertebral disc. A change in intradiscal pressure (osmotic change) or inflammatory cytokines may also be involved. Further studies are needed to examine the interplay of various Wnt ligands, other signaling pathways (e.g., non-Smad pathways), and osmolarity in the intervertebral disc, and whether these can modulate Wnt signaling.

ACKNOWLEDGMENTS

We greatly appreciate the helpful advice from and excellent technical assistance of Tadayuki Sato and Mayumi Nakano. We also thank Dr. Koichiro Abe for providing tissue samples. Animal experiments were carried out according to a protocol approved by the Animal Experimentation Committee at our institution. This study was supported by The Japan Orthopaedics and Traumatology Foundation (0120) and a Grant-in-Aid for Scientific Research and a Grant of The Science Frontier Program from the Ministry of Education, Culture, Sports, Science, and Technology of Japan.

REFERENCES

Alonso M, Martinez A. 2004. GSK-3 inhibitors: Discoveries and developments. Curr Med Chem 11:755–763.

Amati B, Land H. 1994. Myc-Max-Mad: A transcription factor network controlling cell cycle progression, differentiation and death. Curr Opin Genet Dev 4:102–108.

Behrens J, von Kries JP, Kühl M, Bruhn L, Wedlich D, Grosschedl R, Birchmeier W. 1996. Functional interaction of β-catenin with the transcription factor LEF-1. Nature 382:638–642.

Behrens J, Jerchow BA, Würtele M, Grimm J, Asbrand C, Wirtz R, Kühl M, Wedlich D, Birchmeier W. 1998. Functional interaction of an axin homolog, conductin, with (-catenin, APC, and GSK3). Science 280:596–599.

Berridge MJ, Downes CP, Hanley MR. 1982. Lithium amplifies agonist-dependent phosphatidylinositol responses in brain and salivary glands. Biochem J 206:587–595.

Bouchard C, Staller P, Eilers M. 1998. Control of cell proliferation by Myc. Trends Cell Biol 8(5):202–206.

Cadigan KM, Nusse R. 1997. Wnt signaling: A common theme in animal development. Genes Dev 11:3286–3305.

Clevers H, van de Wetering M. 1997. TCF/LEF factor earn their wings. Trends Genet 13:485–489.

He TC, Sparks AB, Rago C, Hermeking H, Zawel L, da Costa LT, Morin PJ, Vogelstein B, Kinzler KW. 1998. Identification of c-MYC as a target of the APC pathway. Science 281:1509–1512.

Hiyama A, Mochida J, Iwashina T, Omi H, Watanabe T, Serigano K, Iwabuchi S, Sakai D. 2007. Synergistic effect of low-intensity pulsed ultrasound on growth factor stimulation of nucleus pulposus cells. J Orthop Res 25:1574–1581.

Hiyama A, Mochida J, Iwashina T, Omi H, Watanabe T, Serigano K, Tamura F, Sakai D. 2008. Transplantation of mesenchymal stem cells in a canine disc degeneration model. J Orthop Res 26:589–600.

Hiyama A, Sakai D, Risbud MV, Tanaka M, Arai F, Abe K, Mochida J. 2010. Enhancement of intervertebral disc cell senescence by WNT/β-catenin signaling-induced matrix metalloproteinase expression. Arthritis Rheum 62:3036–3047.

Hiyama A, Sakai D, Tanaka M, Arai F, Nakajima D, Abe K, Mochida J. 2011. The relationship between the Wnt/β-catenin and TGF-β/BMP signals in the intervertebral disc cell. J Cell Physiol 226:1139–1148.

Huang MJ, Cheng YC, Liu CR, Lin S, Liu HE. 2006. A small-molecule c-Myc inhibitor, 10058-F4, induces cell-cycle arrest, apoptosis, and myeloid differentiation of human acute myeloid leukemia. Exp Hematol 34:1480–1489.

Hueber AO, Zörnig M, Lyon D, Suda T, Nagata S, Evan GI. 1997. Requirement for the CD95 receptor-ligand pathway in c-Myc-induced apoptosis. Science 278:1305–1309.

Kikuchi A, Kishida S, Yamamoto H. 2006. Regulation of Wnt signaling by protein–protein interactions and post-translational modifications. Exp Mol Med 38:1–10.

Korinek V, Barker N, Morin PJ, van Wichen D, de Weger R, Kinzler KW, Vogelstein B, Clevers H. 1997. Constitutive transcriptional activation by a β-catenin-Tcf complex in $APC^{-/-}$ colon carcinoma. Science 275:1784–1787.

Logan CY, Nusse R. 2004. The Wnt signaling pathway in development and disease. Annu Rev Cell Dev Biol 20:781–810.

Madiehe AM, Mampuru LJ, Tyobeka EM. 1995. Induction of apoptosis in HL-60 cells by lithium. Biochem Biophys Res Commun 209:768–774.

Mateyak MK, Obaya AJ, Adachi S, Sedivy JM. 1997. Phenotypes of c-Myc-deficient rat fibroblasts isolated by targeted homologous recombination. Cell Growth Differ 8:1039–1048.

Mazumdar J, O'Brien WT, Johnson RS, LaManna JC, Chavez JC, Klein PS, Simon MC. 2010. O_2 regulates stem cells through Wnt/β-catenin signalling. Nat Cell Biol 12:1007–1013.

Meijer L, Flajolet M, Greengard P. 2004. Pharmacological inhibitors of glycogen synthase kinase 3. Trends Pharmacol Sci 25:471–480.

Morin PJ, Sparks AB, Korinek V, Barker N, Clevers H, Vogelstein B, Kinzler KW. 1997. Activation of β-catenin-Tcf signaling in colon cancer by mutations in β-catenin or APC. Science 275:1787–1790.

Reinhold MI, Kapadia RM, Liao Z, Naski MC. 2006. The Wnt-inducible transcription factor Twist1 inhibits chondrogenesis. J Biol Chem 281: 1381–1388.

Reya T, Clevers H. 2005. Wnt signalling in stem cells and cancer. Nature 434:843–850.

Schreiber-Agus N, DePinho RA. 1998. Repression by the Mad (Mxi1)-Sin3 complex. BioEssays 20:808–818.

Spencer GJ, Utting JC, Etheridge SL, Arnett TR, Genever PG. 2006. Wnt signalling in osteoblasts regulates expression of the receptor activator of NFκB ligand and inhibits osteoclastogenesis in vitro. J Cell Sci 119:1283–1296.

Stambolic V, Ruel L, Woodgett JR. 1996. Lithium inhibits glycogen synthase kinase-3 activity and mimics wingless signalling in intact cells. Curr Biol 6:1664–1668.

Trout JJ, Buckwalter JA, Moore KC, Landas SK. 1982. Ultrastructure of the human intervertebral disc. I. Changes in notochordal cells with age. Tissue Cell 14:359–369.

Watanabe T, Sakai D, Yamamoto Y, Iwashina T, Serigano K, Tamura F, Mochida J. 2010. Human nucleus pulposus cells significantly enhanced biological properties in a coculture system with direct cell-to-cell contact with autologous mesenchymal stem cells. J Orthop Res 28:623–630.

Weng LH, Wang CJ, Ko JY, Sun YC, Wang FS. 2010. Control of Dkk-1 ameliorates chondrocyte apoptosis, cartilage destruction, and subchondral bone deterioration in osteoarthritic knees. Arthritis Rheum 62:1393–1402.

Yin X, Giap C, Lazo JS, Prochownik EV. 2003. Low molecular weight inhibitors of Myc–Max interaction and function. Oncogene 22: 6151–6159.

Zhu M, Tang D, Wu Q, Hao S, Chen M, Xie C, Rosier RN, O'Keefe RJ, Zuscik M, Chen D. 2009. Activation of β-catenin signaling in articular chondrocytes leads to osteoarthritis-like phenotype in adult β-catenin conditional activation mice. J Bone Miner Res 24:12–21.

Zindy F, Eischen CM, Randle DH, Kamijo T, Cleveland JL, Sherr CJ, Roussel MF. 1998. Myc signaling via the ARF tumor suppressor regulates p53-dependent apoptosis and immortalization. Genes Dev 12:2424–2433.

ARTHRITIS & RHEUMATISM
Vol. 63, No. 5, May 2011, pp 1355–1364
DOI 10.1002/art.30246

Hypoxia Activates the Notch Signaling Pathway in Cells of the Intervertebral Disc

Implications in Degenerative Disc Disease

Akihiko Hiyama,[1] Renata Skubutyte,[2] Dessislava Markova,[2] D. Greg Anderson,[2] Sanjay Yadla,[2] Daisuke Sakai,[3] Joji Mochida,[3] Todd J. Albert,[2] Irving M. Shapiro,[2] and Makarand V. Risbud[2]

Objective. **To investigate whether hypoxia regulates Notch signaling, and whether Notch plays a role in intervertebral disc cell proliferation.**

Methods. **Reverse transcription–polymerase chain reaction and Western blotting were used to measure expression of Notch signaling components in intervertebral disc tissue from mature rats and from human discs. Transfections were performed to determine the effects of hypoxia and Notch on target gene activity.**

Results. **Cells of the nucleus pulposus and annulus fibrosus of rat disc tissue expressed components of the Notch signaling pathway. Expression of Notch-2 was higher than that of the other Notch receptors in both the nucleus pulposus and annulus fibrosus. In both tissues, hypoxia increased Notch1 and Notch4 messenger RNA (mRNA) expression. In the annulus fibrosus, mRNA expression of the Notch ligand Jagged1 was induced by hypoxia, while Jagged2 mRNA expression was highly sensitive to hypoxia in both tissues. A Notch signaling inhibitor, L685458, blocked hypoxic induction of the activity of the Notch-responsive luciferase reporters 12xCSL and CBF1. Expression of the Notch target gene Hes1 was induced by hypoxia, while coexpression with the Notch–intracellular domain increased Hes1 promoter activity. Moreover, inhibition of Notch signaling blocked disc cell proliferation. Analysis of human disc tissue showed that there was increased expression of Notch signaling proteins in degenerated discs.**

Conclusion. **In intervertebral disc cells, hypoxia promotes expression of Notch signaling proteins. Notch signaling is an important process in the maintenance of disc cell proliferation, and thus offers a therapeutic target for the restoration of cell numbers during degenerative disc disease.**

The intervertebral disc is a specialized tissue that permits rotation, as well as flexure and extension, of the spine. One overriding aspect of disc cell biology is that cells of the nucleus pulposus and cells residing in the inner annulus are removed from the blood supply (1). For example, blood vessels originating in the vertebral body traverse the superficial region of the end plates; none of these vessels infiltrate the nucleus pulposus. With respect to the annulus, this tissue is considered to be avascular, except for small discrete capillary beds present in the dorsal and ventral surfaces; in no case does the annulus vasculature enter the nucleus pulposus (2–4). Modeling studies by Bartels and colleagues indicate that the Po_2 levels within the disc are low (5); related to this observation, cells in the transitional zone between the inner annulus and the nucleus, as well as in the nucleus itself, display a robust hypoxic signal (6). In line with the avascular nature of this tissue, there is a robust and constitutive expression of both hypoxia-inducible factor 1α (HIF-1α) and HIF-2α, confirming that the inner annulus and nucleus pulposus cells reside in a hypoxic environment (7–9).

Supported by the NIH (grants R01-AR-050087 to Drs. Shapiro and Risbaud and R01-AR-055655 to Dr. Risbud).

[1]Akihiko Hiyama, MD, PhD: Thomas Jefferson University, Philadelphia, Pennsylvania and Tokai University School of Medicine, Kanagawa, Japan; [2]Renata Skubutyte, MS, Dessislava Markova, PhD, D. Greg Anderson, MD, Sanjay Yadla, MD, Todd J. Albert, MD, Irving M. Shapiro, PhD, Makarand V. Risbud, PhD: Thomas Jefferson University, Philadelphia, Pennsylvania; [3]Daisuke Sakai, MD, PhD, Joji Mochida, MD: Tokai University School of Medicine, Kanagawa, Japan.

Address correspondence to Makarand V. Risbud, PhD, Department of Orthopaedic Surgery, Thomas Jefferson University, 1015 Walnut Street, Suite 501 Curtis Building, Philadelphia, PA 19107. E-mail: makarand.risbud@jefferson.edu.

Submitted for publication October 12, 2010; accepted in revised form January 6, 2011.